

General Disclaimer

One or more of the Following Statements may affect this Document

- This document has been reproduced from the best copy furnished by the organizational source. It is being released in the interest of making available as much information as possible.
- This document may contain data, which exceeds the sheet parameters. It was furnished in this condition by the organizational source and is the best copy available.
- This document may contain tone-on-tone or color graphs, charts and/or pictures, which have been reproduced in black and white.
- This document is paginated as submitted by the original source.
- Portions of this document are not fully legible due to the historical nature of some of the material. However, it is the best reproduction available from the original submission.

11176-H080-R0-00

APOLLO LM AND CSM S-BAND ANTENNA TRACKING STUDIES
TASK E-53C-1
TECHNICAL REPORT

NAS9-8166

2 December 1968

CSM-HGA INTERCHANGEABILITY STUDY
ANTENNA AND RF CIRCUITRY ANALYSIS

Prepared For

NATIONAL AERONAUTICS AND SPACE ADMINISTRATION
MANNED SPACECRAFT CENTER
HOUSTON, TEXAS

FACILITY FORM 602

N 69-18195
(ACCESSION NUMBER)

37
(PAGES)

NASA-CR-99500
(NASA CR OR TMX OR AD NUMBER)

(THRU) **7**

(CODE)

(CATEGORY) **07**

TRW
SYSTEMS GROUP

NASA CR 99500

11176-H080-R0-00

APOLLO LM AND CSM S-BAND ANTENNA TRACKING STUDIES

CSM-HGA INTERCHANGEABILITY STUDY
ANTENNA AND RF CIRCUITRY ANALYSIS

TASK E-53C-1

Prepared by

Jimmie D. Osborn

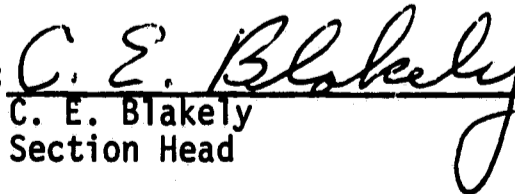
2 December 1968

Approved by:



Jack W. Pool
Task Manager, E-53C-1

Approved by:



C. E. Blakely
Section Head

Approved by:



J. DeVillier, Manager
Communication and Sensor Systems
Department

TRW
SYSTEMS GROUP

TABLE OF CONTENTS

		Page
1.0	INTRODUCTION.	1
2.0	ANTENNA SYSTEMS OPERATIONAL DESCRIPTION	4
3.0	RF SUBSYSTEM MATH MODEL DEVELOPMENT	13
	3.1 General Model.	13
	3.2 Near Boresight Model	21
	3.3 Critical Parameters That Affect Interchange- ability.	26
4.0	EFFECT OF THE IN-LINE TEST PROCEDURE ON INTERCHANGE- ABILITY	28
	4.1 Boresight Alignment With An Electronics Assembly	28
	4.2 Boresight Alignment Without An Electronics Assembly	28
	4.3 Percent Modulation Slope Adjustment With An Apollo Receiver.	28
	4.4 Percent Modulation Slope Adjustment Without An Apollo Receiver.	29
5.0	PROCEDURE FOR DETERMINING INTERCHANGEABILITY.	30
	5.1 Format for the Interchangeability Study Output . .	30
	5.2 Use of the RF Mathematical Model	30
	5.3 Use of the In-Line Test Procedure.	33
6.0	CONCLUSIONS	34
APPENDIX		
	A. Math Model Computer Program Listing	A-1
	REFERENCES	R-1

LIST OF ILLUSTRATIONS

	Page
1. CSM-HGA System.	5
2. Aperture Distribution for One CSM Parabola.	6
3. CSM-HGA RF Circuitry.	7
4. Basic Comparator Circuit.	8
5. Directional Coupler Operation	10
6. Math Model Comparator Circuit Schematic	14
7. Vector Addition of Sum and Difference Voltage	25
8. Narrow Mode Transfer Functions.	31
9. Wide Mode Transfer Functions.	32

TABLES

1. Beam Switching Logic	11
2. Sum Error Sources	18
3. Difference Error Sources.	19

1.0 INTRODUCTION

The Apollo Command Service Module (CSM) S-Band High Gain Antenna (HGA) System, which is used for CSM-earth communications, consists of two sequentially lobed monopulse antennas that are pointed by tracking an earth transmitter. Due to scheduling problems, the various subsystems that comprise the CSM-HGA system are not tested as a complete system until final assembly at the launch site. Therefore, it is necessary that each subsystem be manufactured and tested to rigorous specifications so that satisfactory overall system performance can be guaranteed prior to final assembly. In effect, the subsystems assigned a particular serial number HGA system will be interchangeable with the subsystems of other serial numbered HGA systems. To determine the extent of the added requirements for interchangeability, it is necessary to first accurately describe the subsystem transfer function characteristics mathematically and then, using these expressions, analytically determine the interchangeability requirements.

The purpose of this report is to present a mathematical model of the RF portion of the Apollo High Gain Antenna System and to outline an approach to determining the interchangeability of CSM-HGA RF subsystems. Since the output of a sequentially lobed antenna system is an amplitude modulated voltage whose index of modulation is a function of the space angle, the antenna parameters that determine interchangeability are boresight alignment and variation in index of modulation from unit to unit.

The index of modulation slope near the antenna boresight is referred to as antenna transfer function or antenna gain constant. A mathematical model of the RF system has been developed for the purpose of isolating critical circuit components and predicting RF boresight shift and index of modulation variations caused by manufacturing tolerances and temperature differentials. The model is also used to predict the effects of crosstalk between wide and narrow beam modes. Manufacturing tolerances are compensated for in the in-line test procedure, Dalmo Victor Report No. 15786, "Microwave In-Line Test Procedure for Apollo CSM High Gain Antenna", dated October 11, 1966. Interchangeability is determined by the accuracy of the test procedures combined with the boresight shift and variation in index of

modulation caused by temperature differentials in the operational environment. The approach to the study of RF subsystem interchangeability is as follows:

1. Develop a mathematical model of the RF system that includes amplitude and phase errors from each RF component.
2. Reduce the model to a simplified form (near boresight model) to isolate critical circuit components.
3. Calculate the RF component adjustment range required to compensate for manufacturing tolerances (where adjustments are called for in the in line test procedures).
4. Calculate the boresight shift and variation in index of modulation caused by temperature differentials in the operational environment.
5. Determine the effects of crosstalk between operating modes.
6. Determine the accuracy of boresight alignment resulting from the in-line test procedures.
7. Determine the accuracy of antenna gain constant from the in-line test procedures.
8. Combine the results of the above to determine an antenna system transfer function envelope for use in a total system interchangeability analysis.

The following sections of this report cover items 1 and 2 above. Section 2.0 outlines the RF sub-system tracking operation. A description of the antenna system and comparator circuitry is included.

Section 3.0 presents the mathematical model development. This section not only presents the general model but a near boresight, simplified math model that reveals the first order error sources in the system.

Section 4.0 reviews the major in-line test procedures and assembly techniques used by the manufacturer of the CSM HGA system and discusses the major effect of these procedures.

Section 5.0 presents a method for determining RF subsystem interchangeability. This method involves the use of the mathematical model developed here, a computer program, and the major in-line test procedures. These tools will be instrumental in determining the transfer function envelope of the RF subsystem that will insure interchangeability. This method will be utilized in the further investigation of RF subsystem interchangeability and the results will be published in a later report.

2.0 ANTENNA SYSTEMS OPERATIONAL DESCRIPTION

The HGA System consists of two four-element phase monopulse arrays that are used to generate a broad antenna beam for acquisition and a narrow beam for tracking. As shown in Figure 1, the narrow beam array consists of four parabolic reflectors and the wide mode array is four cross-dipoles located at the center of the array of parabolas. The parabolas appear to have squinted feeds as is typical of an amplitude monopulse system; however, the dipole feed elements are not displaced from the parabola focal points. The dipole elements have been rotated about the reflector focal point which produces an aperture distribution that is skewed toward the center of the array as shown in Figure 2. This moves the effective phase center of each parabola closer to the center of the array and produces a near optimum phase center separation. Other effects such as secondary pattern asymmetry are second order to the antenna operation.

The RF comparator circuitry is a conventional monopulse circuit with lobing switches added for the purpose of modulating the sum pattern with the elevation and azimuth difference patterns. This is, in effect, sequential lobing, but the system is still basically monopulse in that it seeks the azimuth and elevation difference pattern nulls and can be analyzed in nearly the same manner as a monopulse system¹. The primary advantage of the sequentially lobed tracker over the conventional phase monopulse tracker is that a single receiver is required in the first case while three phase matched receivers are required in the second. As shown in Figure 3, the essential parts of the RF comparator circuitry are the wide beam comparator, narrow/medium beam comparator, and mode switch. Four hybrid rings comprise the comparator circuit that generates the monopulse sum (Σ) and difference (Δ) patterns in the wide or narrow beam mode. The difference pattern is added to the sum pattern in the directional coupler, and the lobing switches determine which difference pattern is added at a particular time. Both the narrow and broad beam modes use the same basic comparator circuit, however, the narrow mode circuit has two additional diode switches in the "d" element circuit. The purpose of these are to isolate the "d" parabola for the medium beam transmit mode. The basic comparator circuit is shown in Figure 4 where the antenna elements are denoted as A, B, C and

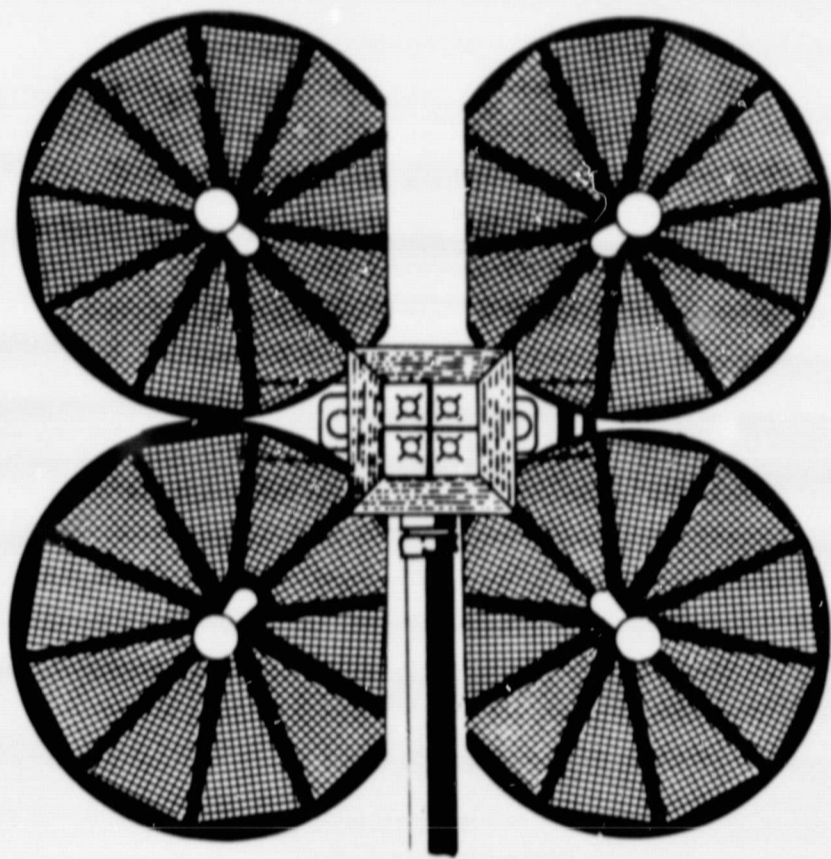


Figure 1. CSM-HGA Antenna System

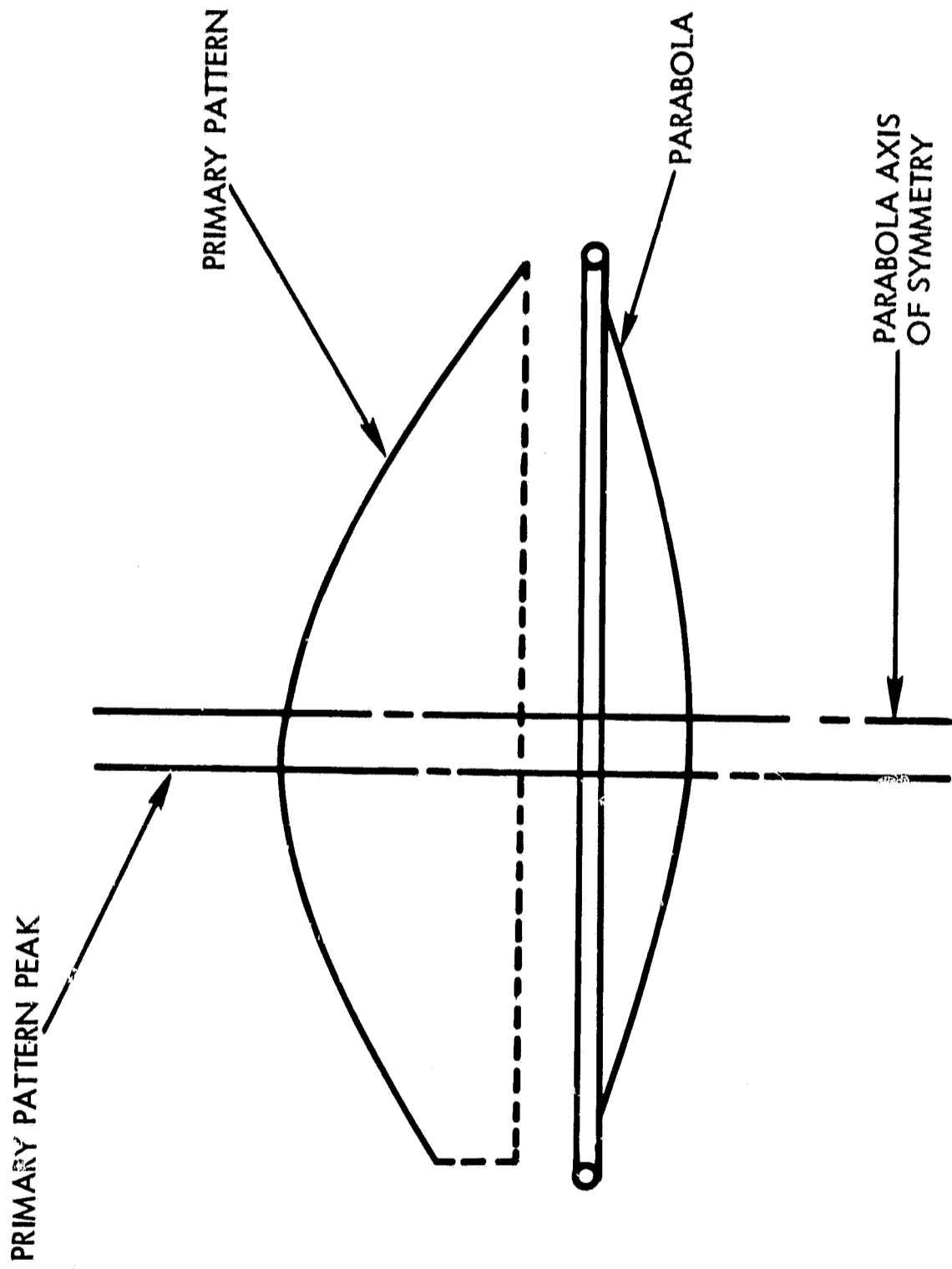


Figure 2. Aperture Distribution for One CSM Parabola

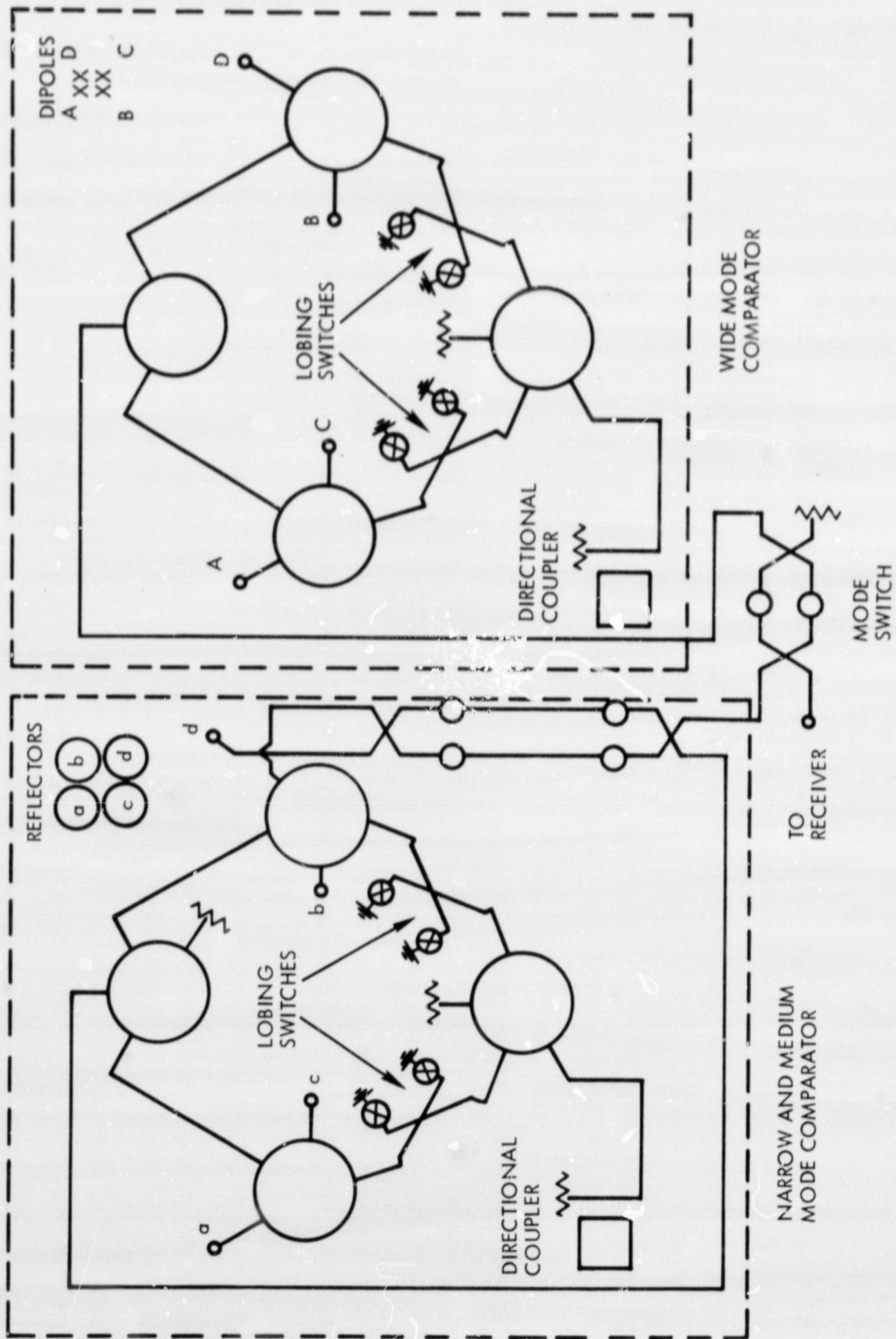


Figure 3.. CSM-HGA RF Circuitry

ANTENNA
CONFIGURATION

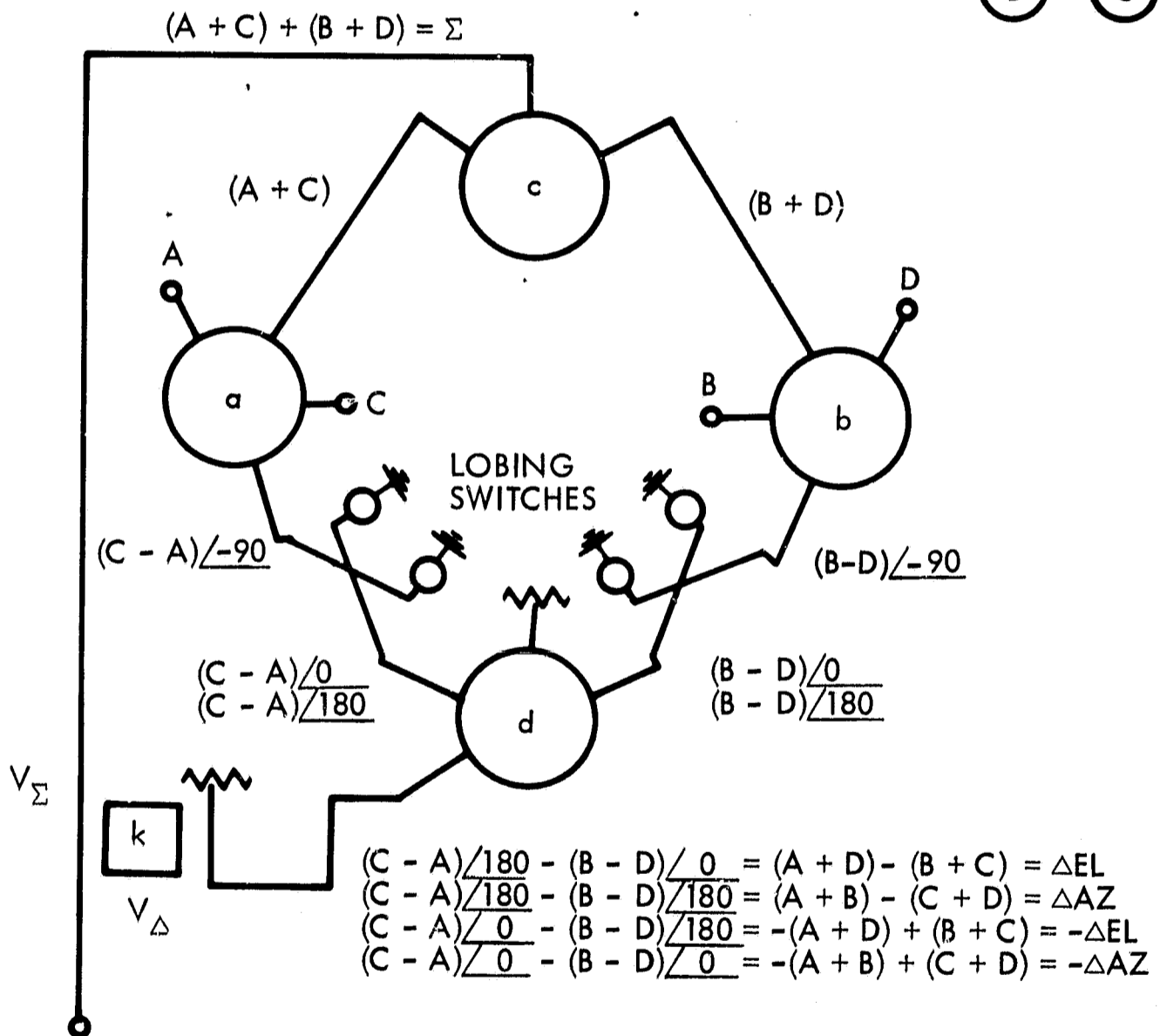
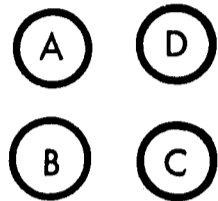


Figure 4. Basic Comparator Circuit

D. Antennas A and C are arrayed in phase in hybrid "a" to yield $(A + C)$, and B and D are arrayed in phase in hybrid "b" to yield $(B + D)$. $(A + C)$ and $(B + D)$ are arrayed in phase in hybrid "c" resulting in the sum pattern $(A + C) + (B + D)$ at the "c" hybrid output. This part of the comparator circuit is typical of a phase monopulse tracking system.¹ The difference output of hybrids "a" and "b" are $(C - A)$ and $(B - D)$, respectively. To obtain sequential lobing, the "a" and "b" hybrid difference outputs are shifted by 0 or 180 degrees by the lobing switches before $(B - D)$ is subtracted from $(C - A)$ in the "d" hybrid. If the inputs to hybrid "d" are $(C - A) / \underline{180^\circ}$ and $(B - D) / \underline{0^\circ}$, the output is the elevation pattern $(A + D) - (B + C)$. If the inputs are $(C - A) / \underline{180^\circ}$ and $(B - D) / \underline{180^\circ}$, the output is the azimuth difference pattern $(A + B) - (C + D)$. The negative elevation and azimuth difference patterns are obtained from the remaining two possible switch conditions. The four outputs corresponding to the four input phase relationships are listed in Figure 4.0.

The operation of the lobing switches is best explained by considering the operation of the directional couplers in the switching circuitry under shorted and open terminal conditions. In Figure 5 (a), the switch between the "a" and "d" hybrids is shown with the diodes reversed biased, i.e., the directional coupler is terminated in an open circuit. The coupler has a 3 dB coupling coefficient, therefore, one half of the input power is directed toward each diode and is reflected back by an open circuit which results in no relative phase shift. Since the coupling section of the coupler is a quarter wavelength long, the reflection from each diode is delayed by 90 degrees and is in phase at the output terminal. This results in all the input power directed toward the output terminal, or, the output is $(C - A) / \underline{0^\circ}$. If, as in Figure 5. (b), the diodes are forward biased, the coupler is terminated in a short and the diode reflections are now reversed in phase resulting in a 180 degree phase shift relative to the open circuit case. By referring to the diode bias information in Figure 5, the comparator output and beam position can be determined for each diode bias condition. In Table 1, the four possible beam positions are tabulated. The beam is scanned clockwise and the driving function is determined by moving from top to bottom on the table.

If V_Σ and V_Δ are vector voltage expressions proportional to the actual voltage generated at the sum and difference terminals, as defined

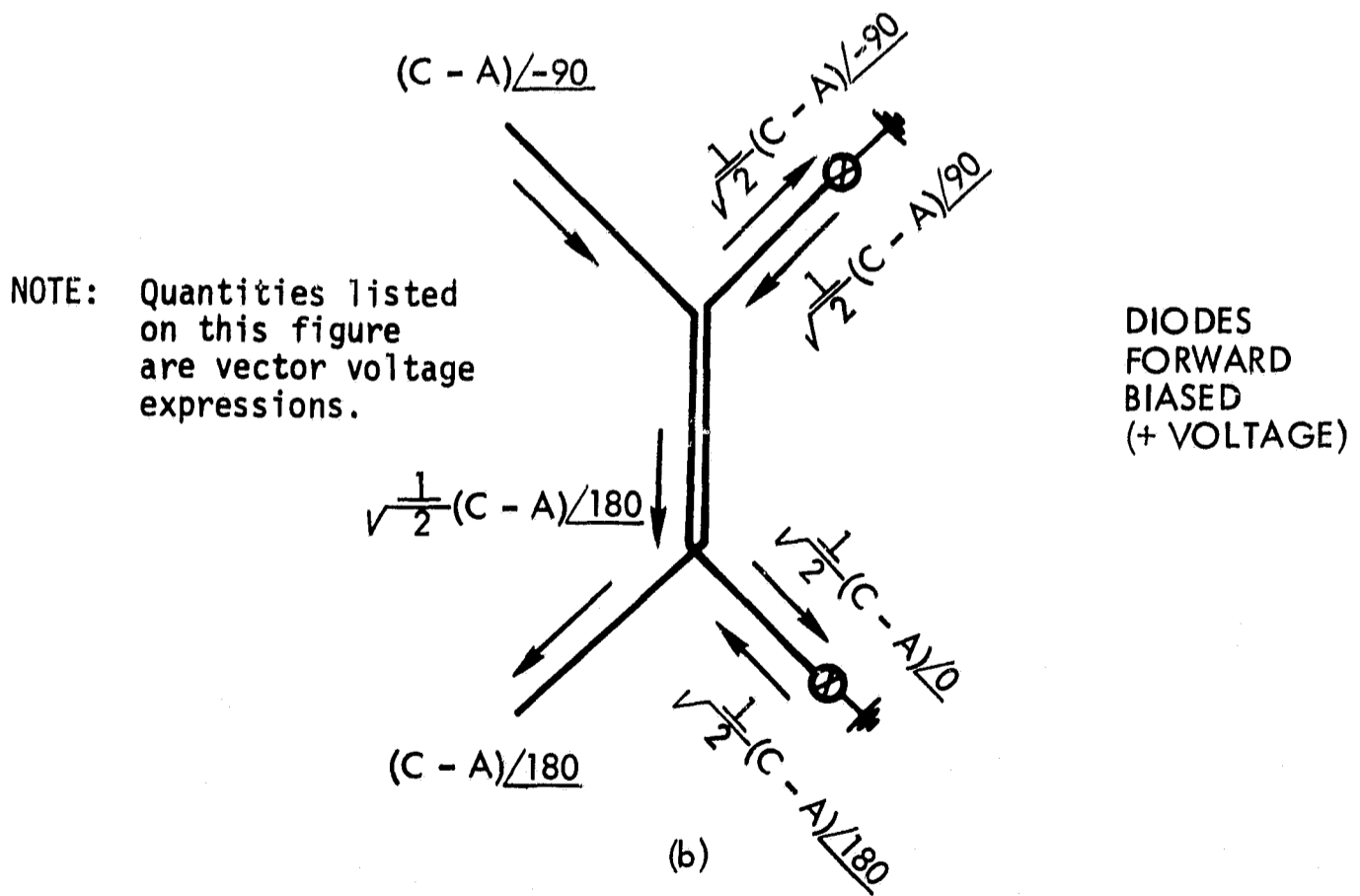
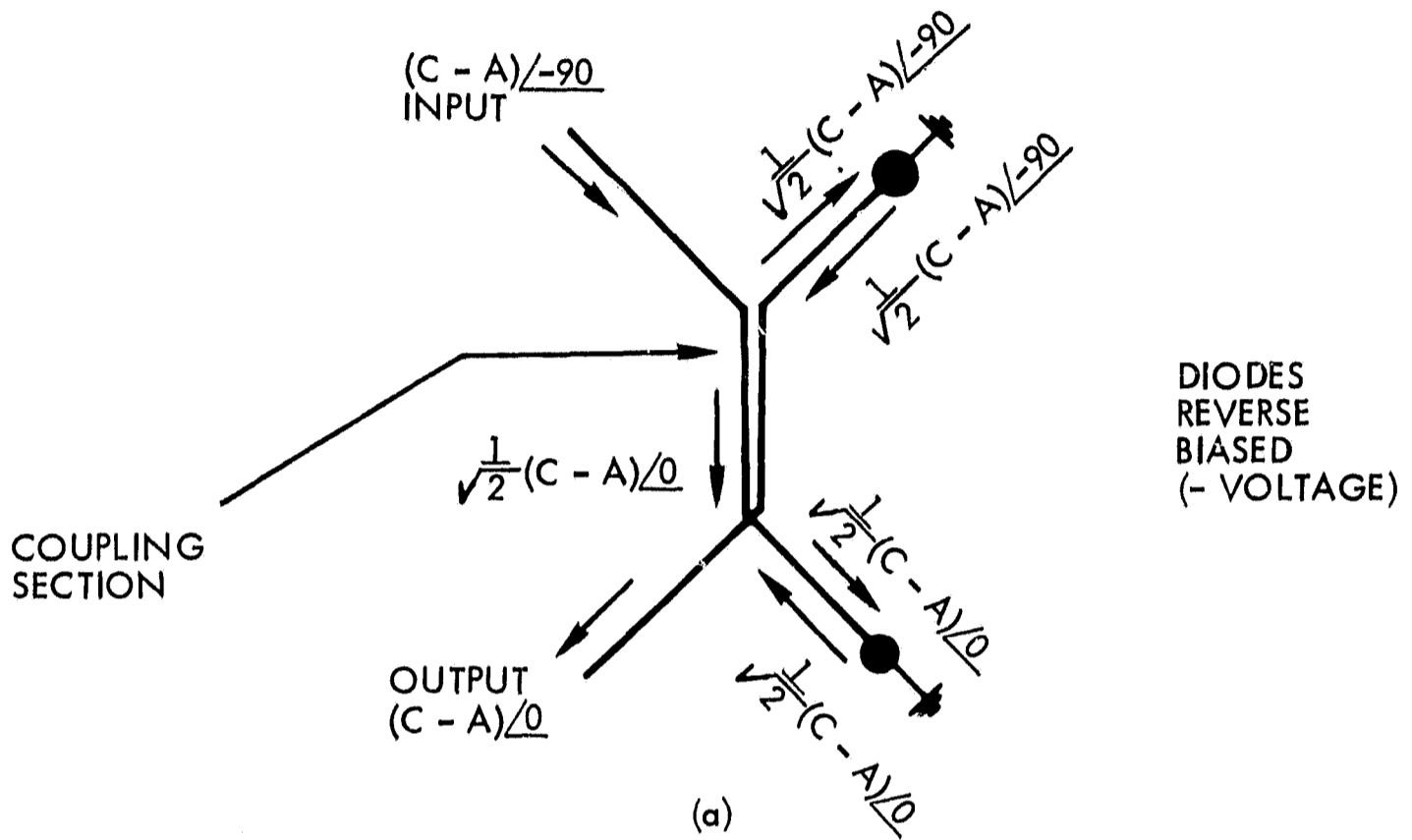


Figure 5. Directional Coupler Operation

DIODE BIAS (VOLTAGE)		COMPARATOR OUTPUT	BEAM POSITION
LEFT SWITCH	RIGHT SWITCH		
+	-	$\Sigma + \Delta EL$	UP
+	+	$\Sigma + \Delta AZ$	RIGHT
-	+	$\Sigma - \Delta EL$	DOWN
-	-	$\Sigma - \Delta AZ$	LEFT

+ INDICATES A POSITIVE DIODE VOLTAGE
 - INDICATES A NEGATIVE DIODE VOLTAGE

Table 1. Beam Switching Logic

in Figure 4., the index of modulation is given by²

$$m_i = \frac{|V_{\Sigma} + V_{\Delta}| - |V_{\Sigma} - V_{\Delta}|}{|V_{\Sigma} + V_{\Delta}| + |V_{\Sigma} - V_{\Delta}|} \quad (1)$$

This can also be represented in terms of beam position if V_R and V_L are the comparator output voltages for the beam switched in the right and left positions, respectively. In this case

$$m_i = \frac{|V_R| - |V_L|}{|V_R| + |V_L|} \quad (2)$$

or if the elevation plane is used,

$$m_i = \frac{|V_U| - |V_D|}{|V_U| + |V_D|} \quad (3)$$

where the U and D subscripts represent the up and down beam switched positions.

3.0 RF SUBSYSTEM MATH MODEL DEVELOPMENT

The mathematical model of the RF circuitry was developed by writing RF voltage equations at various points in the circuit and combining them at the comparator output to give an expression for index of modulation. General amplitude and phase errors are included in the equations to account for errors from each RF component. Antenna element patterns can be included in the equations, and the model will present an accurate description of RF system performance over a wide range of space angles. To determine the critical parameters when the system is tracking on RF boresight, the model is reduced to a simple form by using small angle approximations. The simplified model, although it is restricted to angles near boresight, presents an uncluttered mathematical description of the system while a computer solution is required for the general model. Since the RF circuitry for the broad and narrow beam tracking modes is basically the same, one model is used for both modes.

Due to the similarities in the Apollo CSM-HGA and Lunar Module (LM) steerable antenna system, it should be noted that the mathematical model in this report can be readily modified to represent the LM steerable antenna subsystem.

3.1 General Model

As shown in Figure 6., the circuit used in the model is a conventional monopulse comparator with the lobing or beamswitching circuitry added to it. If E_A , E_B , E_C and E_D are the principle plane radiation patterns for antennas A, B, C and D, the voltage at terminal 2 of hybrid "a" is proportional to V_{a2} which is given, for an incident space angle θ , by³

$$V_{a2} = E_A e^{\frac{j\psi_1}{2}} + K_{a2} E_C e^{\frac{-j\psi_1}{2}} \quad (4)$$

(A) (D)
(B) (C)

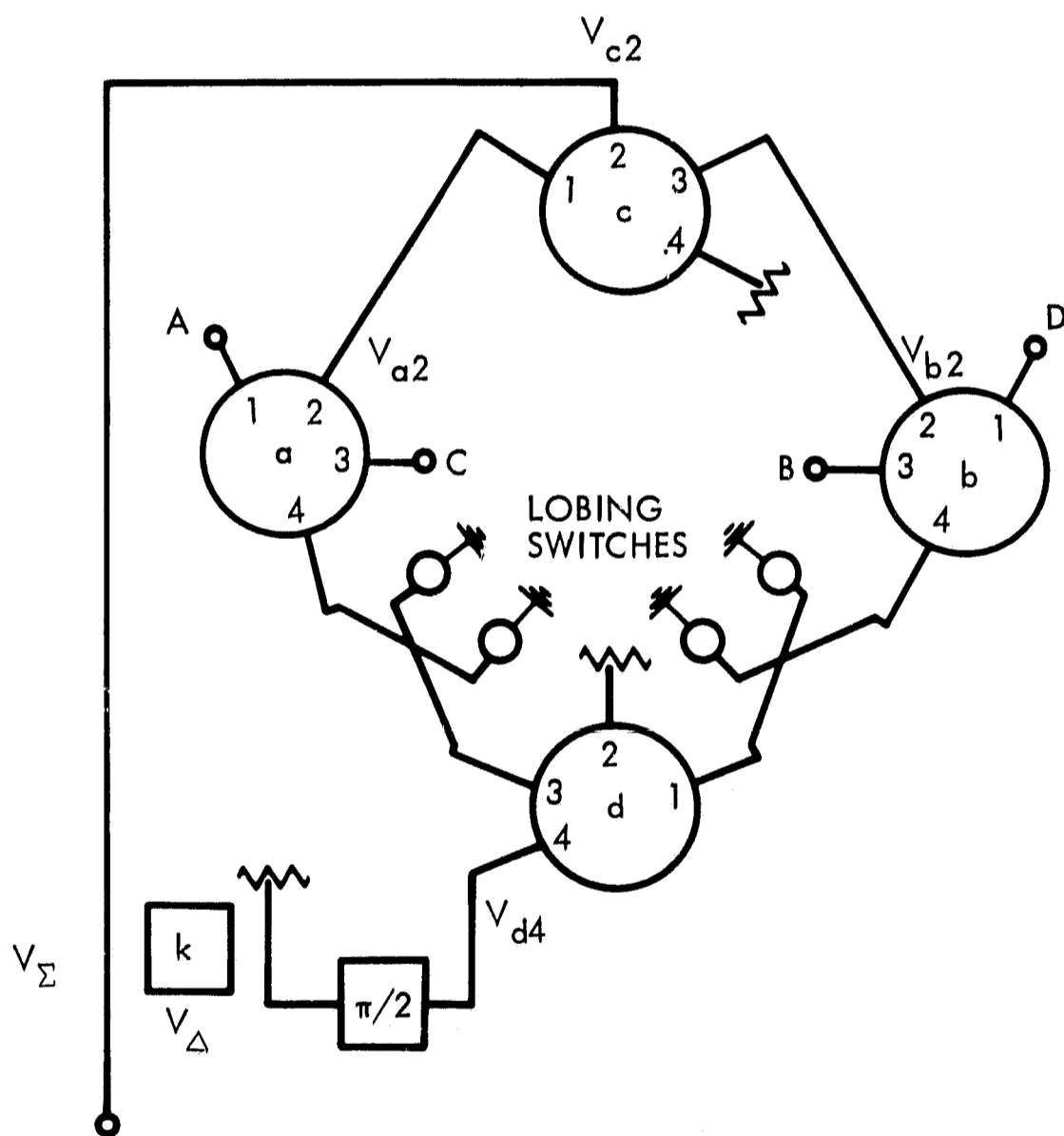


Figure 6. Math Model Comparator Circuit Schematic

where $\psi_1 = \frac{2\pi d}{\lambda} \sin \theta + \delta_{0a} + \delta_{a2}$
 K_{a2} = the amplitude unbalance associated with antennas A and C at terminal 2
 d = antenna phase center separation
 λ = wavelength (RF)
 δ_{0a} = all precomparator phase unbalance associated with hybrid "a"
 δ_{a2} = phase unbalance between antennas A and C associated with hybrid "a" at terminal 2

Similarly, the voltage at terminal 2 of hybrid "b" is proportional to V_{b2} which is given by

$$V_{b2} = E_B e^{\frac{j\psi_2}{2}} + K_{b2} E_D e^{\frac{-j\psi_2}{2}} \quad (5)$$

where $\psi_2 = \frac{2\pi d}{\lambda} \sin \theta + \delta_{0b} + \delta_{b2}$
 K_{b2} = the amplitude unbalance associated with antennas B and D at terminal 2
 δ_{0b} = all precomparator phase unbalance associated with hybrid "b"
 δ_{b2} = phase unbalance between antennas B and D associated with hybrid "b" at terminal 2

Voltages V_{a2} and V_{b2} are combined in hybrid "c" to yield

$$V_{c2} = V_{a2} e^{j\left(\frac{\delta_{TL} + \delta_{c2}}{2}\right)} + K_{c2} V_{b2} e^{-j\left(\frac{\delta_{TL} + \delta_{c2}}{2}\right)} \quad (6)$$

where K_{c2} = the amplitude unbalance from hybrid "c" and associated transmission lines
 δ_{TL} = the phase unbalance in the transmission lines connecting hybrids "a" and "b" to "c"
 δ_{c2} = the phase unbalance in hybrid "c"

V_{c2} is proportional to the sum pattern voltage.

The difference voltage is derived in a similar manner; however, this part of the circuit has the added complexity of the lobing switches. The output of hybrid "a" terminal 4 is given by

$$V_{a4} = -E_A e^{\frac{j\psi_3}{2}} + K_{a4} E_C e^{\frac{-j\psi_3}{2}} \quad (7)$$

where $\psi_3 = \frac{2\pi d}{\lambda} \sin \theta + \delta_{oa} + \delta_{a4}$

δ_{oa} = defined above

δ_{a4} = phase shift between antennas A and C associated with hybrid "a" at terminal 4

The minus sign on E_A occurs because the two antennas are arrayed out of phase in hybrid "a". The output of hybrid "b" is given by

$$V_{b4} = E_B e^{\frac{j\psi_4}{2}} - K_{b4} E_D e^{\frac{-j\psi_4}{2}} \quad (8)$$

where $\psi_4 = \frac{2\pi d}{\lambda} \sin \theta + \delta_{ob} + \delta_{b4}$

δ_{ob} = defined above

δ_{b4} = phase unbalance between antennas B and D associated with hybrid "b" at terminal 4

V_{a4} and V_{b4} are combined in hybrid "d" to yield V_{d4} which is directly related to the difference voltage. Thus,

$$V_{d4} = V_{a4} e^{j\left(\frac{\delta_{DL} + \delta_{sw} + \delta_{d4}}{2}\right)} - K_{d4} V_{b4} e^{-j\left(\frac{\delta_{DL} + \delta_{sw} + \delta_{d4}}{2}\right)} \quad (9)$$

where K_{d4} = the amplitude unbalance from the lobing switches, hybrid "d" and the associated transmission lines
 δ_{DL} = transmission phase unbalance between arms 1 and 3 of hybrid "d"
 δ_{sw} = phase unbalance in the lobing switches
 δ_{b4} = phase unbalance between arms 1 and 3 hybrid "d" at terminal 4

Combining of the error sources occurs in the directional coupler,

$$V_{\Sigma} = K_{LC} V_{c2} e^{j\delta_{LC}} \quad (10)$$

$$V_{\Delta} = jkV_{d4} \quad (11)$$

where k = the coupling coefficient of the directional coupler
 K_{LC} = the amplitude unbalance in the combining circuitry
 δ_{LC} = the phase unbalance in the combining circuitry

If the antenna element patterns are known, the sum voltage V_{Σ} and V_{Δ} can be substituted into the expression for index of modulation which is

$$m_i = \frac{|V_{\Sigma} + V_{\Delta}| - |V_{\Sigma} - V_{\Delta}|}{|V_{\Sigma} + V_{\Delta}| + |V_{\Sigma} - V_{\Delta}|} \quad (12)$$

Substituting Equations 4, 5 and 6 into 10, Equations 7, 8 and 9 into 11 and Equations 10 and 11 into 12, and expression for index of modulation is obtained in terms of the amplitude and phase errors from each RF component. The expression is sufficiently complicated to require a computer solution. The various error sources are tabulated in Tables 2 and 3 where the amplitude unbalances are listed in decibels (dB) and the phase unbalances in degrees. This is done to facilitate the use of available tolerance data on each component. Translating the dB figures into ratios yields

SUM CHANNEL ERROR SOURCES	AMPLITUDE		PHASE	
	SYMBOL	MAGNITUDE (dB)	SYMBOL	MAGNITUDE (DEG)
PRE-COMPARATOR ERRORS BETWEEN ANTENNAS A AND C	Δ_{oa}		δ_{oa}	
PRE-COMPARATOR ERRORS BETWEEN ANTENNAS B AND D	Δ_{ob}		δ_{ob}	
HYBRID "a"	Δ_{a2}		δ_{a2}	
HYBRID "b"	Δ_{b2}		δ_{b2}	
TRANSMISSION LINE BETWEEN PAIRS (A + C) AND (B + D)	Δ_{TL}		δ_{TL}	
HYBRID "c"	Δ_{c2}		δ_{c2}	
TRANSMISSION LINE TO COUPLER	Δ_{LC}		δ_{LC}	

Table 2. Sum Error Sources

DIFFERENCE CHANNEL ERROR SOURCES	AMPLITUDE		PHASE	
	SYMBOL	MAGNITUDE (dB)	SYMBOL	MAGNITUDE (DEG)
PRE-COMPARATOR ERRORS BETWEEN ANTENNAS A AND C	Δ_{oa}		δ_{oa}	
PRE-COMPARATOR ERRORS BETWEEN ANTENNAS B AND D	Δ_{ob}		δ_{ob}	
HYBRID "a"	Δ_{a4}		δ_{a4}	
HYBRID "b"	Δ_{b4}		δ_{b4}	
TRANSMISSION LINE BETWEEN PAIRS (A - C) AND (B - D)	Δ_{TL}		δ_{TL}	
LOBING SWITCH	Δ_{sw}		δ_{sw}	
HYBRID "d"	Δ_{d4}		δ_{d4}	

Table 3. Difference Error Sources

$$K_{a2} = \log^{-1} (\Delta_{oa} + \Delta_{a2})/20 \quad (13)$$

$$K_{b2} = \log^{-1} (\Delta_{ob} + \Delta_{b2})/20 \quad (14)$$

$$K_{c2} = \log^{-1} (\Delta_{TL} + \Delta_{c2})/20 \quad (15)$$

$$K_{LC} = \log^{-1} (\Delta_{LC})/20 \quad (16)$$

$$K_{a4} = \log^{-1} (\Delta_{oa} + \Delta_{a4})/20 \quad (17)$$

$$K_{b4} = \log^{-1} (\Delta_{ob} + \Delta_{b4})/20 \quad (18)$$

$$K_{d4} = \log^{-1} (\Delta_{TL} + \Delta_{sw} + \Delta_{d4})/20 \quad (19)$$

If all error sources are neglected, the expression for m_i reduces to

$$m_i = \frac{V_{\Delta}}{V_{\Sigma}} \quad (20)$$

Substituting expressions for V_{Δ} and V_{Σ} and letting $E_A = E_B = E_C = E_D$, all δ 's = 0, and all K 's = 1, m_i becomes

$$m_i = jk \frac{\left(\frac{j\psi}{2} + e^{-\frac{j\psi}{2}} \right) - \left(\frac{j\psi}{2} - e^{-\frac{j\psi}{2}} \right)}{\left(\frac{j\psi}{2} + e^{-\frac{j\psi}{2}} \right) + \left(\frac{j\psi}{2} + e^{-\frac{j\psi}{2}} \right)} \quad (21)$$

which is equivalent to

$$m_i = k \frac{\sin \frac{\psi}{2}}{\cos \frac{\psi}{2}} \quad (22)$$

or

$$m_i = k \tan \left(\frac{\pi d}{\lambda} \sin \theta \right) \quad (23)$$

Equation 23 is an expression for the index of modulation for a sequentially lobed monopulse antenna system with no amplitude or phase unbalance and is accurate when θ is restricted to within the main beam of the antenna elements that are used in the array.

3.2 Near Boresight Model

From the general model, the sum voltages from hybrids "a" and "b" are

$$V_{a2} = E_A e^{\frac{j\psi_1}{2}} + K_{a2} E_C e^{\frac{-j\psi_1}{2}} \quad (24)$$

and

$$V_{b2} = E_B e^{\frac{j\psi_2}{2}} + K_{b2} E_D e^{\frac{-j\psi_2}{2}} \quad (25)$$

If the space angle θ is restricted so that ψ_1 and ψ_2 are small compared to a radian, these equations can be simplified by using small angle approximations. This is very useful because it results in a simple equation for modulation index m_i , which indicates the critical parameters when the system is actually tracking. If θ is small, and

$$E_A \cong E_C \cong E_B \cong E_D \cong 1 \quad (26)$$

$$K_{a2} \cong K_{b2} \cong K \quad (27)$$

$$\psi_1 \cong \psi_2 \cong \psi \quad (28)$$

are valid approximations, $e^{\frac{j\psi}{2}} \cong 1 + \frac{j\psi}{2}$.

Using this approximate form of $e^{\frac{j\psi}{2}}$

$$V_{a2} \approx 1 + \frac{j\psi}{2} + K(1 - \frac{j\psi}{2}) = (1 + K) + j(1 - K)\frac{\psi}{2} \quad (29)$$

$$V_{b2} \approx 1 + \frac{j\psi}{2} + K(1 - \frac{j\psi}{2}) = (1 + K) + j(1 - K)\frac{\psi}{2} \quad (30)$$

Also, from the general model

$$V_{c2} = V_{a2} e^{\frac{j\delta_s}{2}} + K_{c2} V_{bc} e^{\frac{-j\delta_s}{2}} \quad (31)$$

where $\delta_s = \delta_{TL} + \delta_{c2}$. If the approximate expressions for V_{a2} and V_{b2} are used,

$$V_{c2} \approx \left[(1 + K) + j(1 - K)\frac{\psi}{2} \right] \left(1 + \frac{j\delta_s}{2} \right) + K_{c2} \left[(1 + K) + j(1 - K)\frac{\psi}{2} \right] \left(1 + \frac{j\delta_s}{2} \right) \quad (32)$$

Regrouping,

$$V_{c2} \approx \left[(1 + K)(1 + K_{c2}) - (1 - K)(1 - K_{c2})\frac{\delta_s}{2}\frac{\psi}{2} \right] + j \left[(1 - K)(1 + K_{c2})\frac{\psi}{2} + (1 + K)(1 - K_{c2})\frac{\delta_s}{2} \right] \quad (33)$$

Since K and K_{c2} are approximately unity and both δ_s and ψ are negligible, the expression reduces to

$$V_{c2} \approx (1 + K)(1 + K_{c2}) \quad (34)$$

which indicates that at boresight the sum voltage is essentially constant for $\psi \ll (1 + K)(1 + K_{c2})$.

Again, from the general model, the difference voltages at hybrids "a" and "b" are

$$V_{a4} = -E_A e^{\frac{j\psi_3}{2}} + K_{a4} E_C e^{\frac{-j\psi_3}{2}} \quad (35)$$

and

$$V_{b4} = E_C e^{\frac{j\psi_4}{2}} - K_{b4} E_D e^{\frac{-j\psi_4}{2}} \quad (36)$$

If similar approximations are made in these equations, they reduce to

$$V_{a4} \approx -\left(1 + \frac{j\psi}{2}\right) + K\left(1 - \frac{j\psi}{2}\right) = -(1 - K) - j(1 + K)\frac{\psi}{2} \quad (37)$$

$$V_{b4} \approx \left(1 + \frac{j\psi}{2}\right) - K\left(1 - \frac{j\psi}{2}\right) = (1 - K) + j(1 + K)\frac{\psi}{2} \quad (38)$$

The output of hybrid "d" is

$$V_{d4} = V_{a4} e^{\frac{j\delta_D}{2}} - K_{d4} V_{b4} e^{\frac{-j\delta_D}{2}} \quad (39)$$

where $\delta_D = \delta_{DL} + \delta_{s\omega} + \delta_{d4}$. Substituting the approximate expressions for V_{a4} and V_{b4} yields

$$V_{d4} = \left[-(1 - K) - j(1 + K)\frac{\psi}{2}\right] e^{\frac{j\delta_D}{2}} - K_{d4} \left[(1 - K) + j(1 + K)\frac{\psi}{2}\right] e^{\frac{-j\delta_D}{2}} \quad (40)$$

Regrouping

$$V_{d4} \approx \left[-(1 - K)(1 + K_{d4}) + (1 + K)(1 - K_{d4})\frac{\delta_D}{2} \frac{\psi}{2}\right] \\ - j \left[(1 + K)(1 + K_{d4})\frac{\psi}{2} + (1 - K)(1 - K_{d4})\frac{\delta_D}{2}\right] \quad (41)$$

This equation now reduces to

$$V_{d4} \approx -j(1 + K)(1 + K_{d4})\frac{\psi}{2} \quad (42)$$

The real parts of V_{d4} can be neglected because it is small and is added in phase quadrature with the sum voltage as shown in Figure 7, where the real and imaginary parts of V_{Δ} are shown superimposed upon the sum voltage.

The modulation index,

$$m_i = \frac{|V_{\Sigma} + V_{\Delta}| - |V_{\Sigma} - V_{\Delta}|}{|V_{\Sigma} + V_{\Sigma}| + |V_{\Sigma} - V_{\Delta}|}, \quad (43)$$

reduces to

$$m_i = \frac{V_{\Delta}}{V_{\Sigma}}. \quad (44)$$

If the quadrature components of V_{Σ} and V_{Δ} are neglected,

$$V_{\Sigma} \approx K_{LC} V_{c2} \quad (45)$$

$$V_{\Delta} \approx jkV_{d4} \quad (46)$$

and

$$m_i \approx \frac{jkV_{d4}}{K_{LC} V_{c2}}. \quad (47)$$

Substituting the approximate expressions for V_{c2} and V_{d4} results in

$$m_i \approx \frac{k}{K_{LC}} \left(\frac{1 + K_{d4}}{1 + K_{c4}} \right) \left(\frac{\pi d}{\lambda} \theta + \frac{\delta_{pc}}{2} \right) \quad (48)$$

where δ_{pc} is the total precomparator phase unbalance. Rearranging the constants

$$m_i = \left(\frac{k}{K_{LC}} \right) \left(\frac{1 + K_{d4}}{1 + K_{c4}} \right) \frac{\pi d}{\lambda} \times \theta + \frac{k}{2K_{LC}} \left(\frac{1 + K_{d4}}{1 + K_{c4}} \right) \delta_{pc} \quad (49)$$

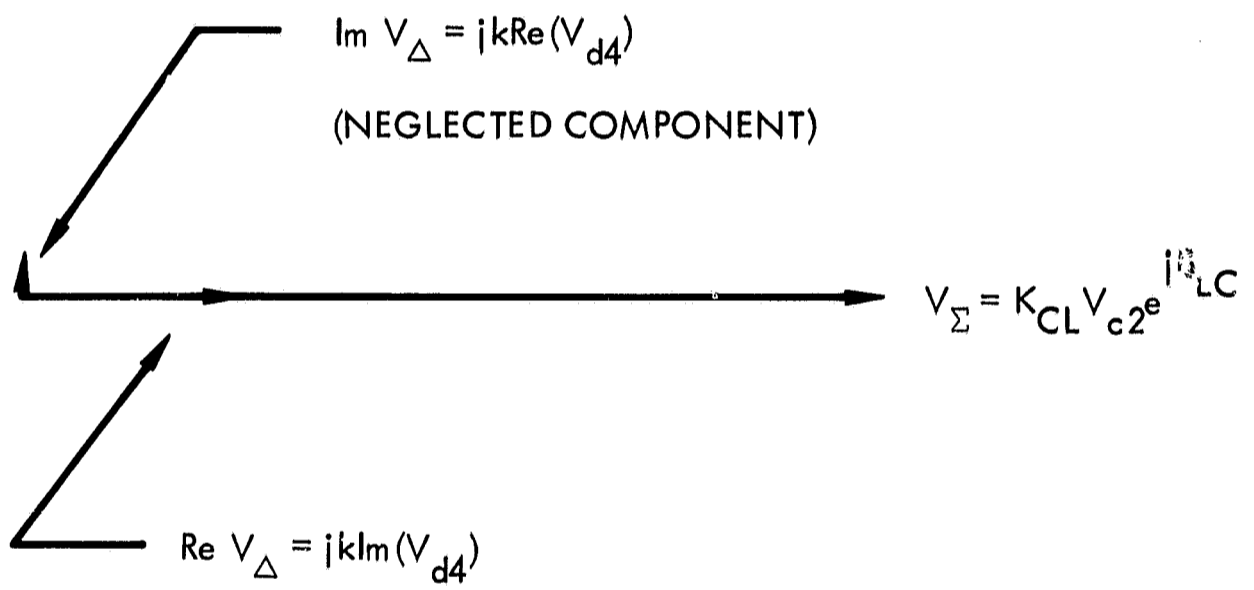


Figure 7. Vector Addition of Sum and Difference Voltage

which is a linear function of θ with a slope determined by the relative amplitudes of the sum and difference voltages, that is, the slope is given by

$$\frac{dm_i}{d\theta} = \left(\frac{k}{K_{LC}} \right) \left(\frac{1 + K_{d4}}{1 + K_{c4}} \right) \frac{\pi d}{\lambda} \quad (50)$$

The slope is dependent upon the various voltage constants k , K_{d4} , K_{c4} and K_{LC} which all relate the relative magnitude of the sum and difference voltages. The boresight shift due to precomparator phase unbalance is found by setting $m_i = 0$ and solving for θ , or

$$\theta_e = - \frac{\delta_{pc}}{2\pi d} \lambda \quad (51)$$

By substituting values measured from actual circuit components, the variation in slope and boresight shift can be determined.

3.3 Critical Parameters That Affect Interchangeability

From Equation 50, the index of modulation slope (for a constant $\frac{d}{\lambda}$) depends on the voltage ratios k , K_{d4} , K_{c4} and K_{LC} . All of these, except k , are very nearly unity and are determined by manufacturing tolerances on the "c" and "d" hybrids and the transmission line between hybrid "c" and the directional coupler. k is, however, the coefficient of coupling for the directional coupler and is adjustable as outlined in the in-line test procedure, making it the most critical parameter in determining the index of modulation slope. From Equation 51, the boresight shift (for a constant $\frac{d}{\lambda}$) depends on precomparator phase shift. Precomparator phase shift caused by manufacturing tolerances on RF components is compensated for in the in-line test procedure by mechanically reorienting the broad beam antenna by using shims at the antenna attach points. Additional precomparator phase shift can occur during actual flight due to temperature differentials between the various antenna transmission lines.

If the less critical parameters are neglected, the expression for index of modulation near boresight is

$$m_i = k \left(\frac{\pi d}{\lambda} \right) \times \theta + \frac{k}{2} \delta_{pc} \quad (52)$$

which reduces the expression for the slope (or antenna gain constant) to

$$\frac{dm_i}{d\theta} = \left(\frac{\pi d}{\lambda}\right) k \quad (53)$$

and boresight error to

$$\theta_e = -\left(\frac{\lambda}{2\pi d}\right) \delta_{pc} \quad (54)$$

These expressions are accurate to within 10 percent up to one degree off boresight in the narrow mode and five degrees in the wide mode.

4.0 EFFECT OF THE IN-LINE TEST PROCEDURE ON INTERCHANGEABILITY

As it is outlined in Section 4.1 through 4.4 of this report, the broad and narrow beam boresights are aligned and the percent modulation slopes are set equal using two different test procedures (i.e., Apollo equipment is used in one procedure while it is not used in the other). The individual antenna element patterns in each array are made to coincide prior to the boresight and slope adjustment by mechanically orienting each element in each array.

4.1 Boresight Alignment With An Electronics Assembly

This procedure utilizes the Dalmo Victor's Antenna System Test Set (ASTS) in conjunction with the electronics assembly to control antenna beam lobing, provide reception, demodulate the error signals and provide an indication of static tracking error on a strip recorder.⁴ Since multipath on the antenna test range affects the wide beam boresight angle, the entire antenna assembly is elevated in increments causing the broad beam null to move cyclically with height, and the average boresight angle then is taken as the true boresight. This average is made to coincide with the narrow beam boresight by mechanically shimming the broad beam antenna to adjust its physical orientation with respect to the narrow beam array.

4.2 Boresight Alignment Without An Electronics Assembly

Without an electronics assembly, the null position cannot be measured directly, so it is determined by measuring the antenna patterns with the beam switched left and then right.⁵ As in Paragraph 4.1, the wide beam boresight is made to coincide with the narrow beam by shimming the broad beam antenna assembly. This procedure is repeated for various antenna heights on the antenna range, and an average shim size is used. A similar technique is used to align the boresight in the orthogonal plane.

4.3 Percent Modulation Slope Adjustment With An Apollo Receiver

In this procedure, the output of an Apollo receiver is monitored for space angles one and five degrees off boresight to determine and adjust the wide and narrow beam percent modulation slopes.⁶ The antenna is first biased for the narrow beam mode, the receiver output is set at a

specified voltage at one degree from boresight by adjusting the narrow beam coupling coefficient k and the voltage at five degrees is recorded. The antenna system is then switched to the broad beam mode, and the receiver output is set equal to the narrow beam output at one and five degrees to within a 5/4 tolerance by adjusting the wide beam coupling coefficient k .

4.4 Percent Modulation Slope Adjustment Without An Apollo Receiver

In this procedure, a standard receiver is used in the test circuit rather than an Apollo receiver.⁷ The antenna is first biased for the broad beam mode, the receiver output is set at a previously specified voltage at one degree from boresight by adjusting the broad beam coupling coefficient k and the voltage at five degrees off boresight is measured. The antenna is then switched to narrow beam, and the receiver output is set equal to the broad beam output at one and five degrees off boresight by adjusting the narrow beam coupling coefficient k and narrow/wide transfer switching phasing.

5.0 PROCEDURE FOR DETERMINING INTERCHANGEABILITY

As discussed in the previous sections, boresight alignment and percent modulation deviation from antenna to antenna will determine interchangeability. The procedure used for determining interchangeability is to predict the maximum deviation in these parameters by using the antenna RF mathematical model and the in-line test procedure.

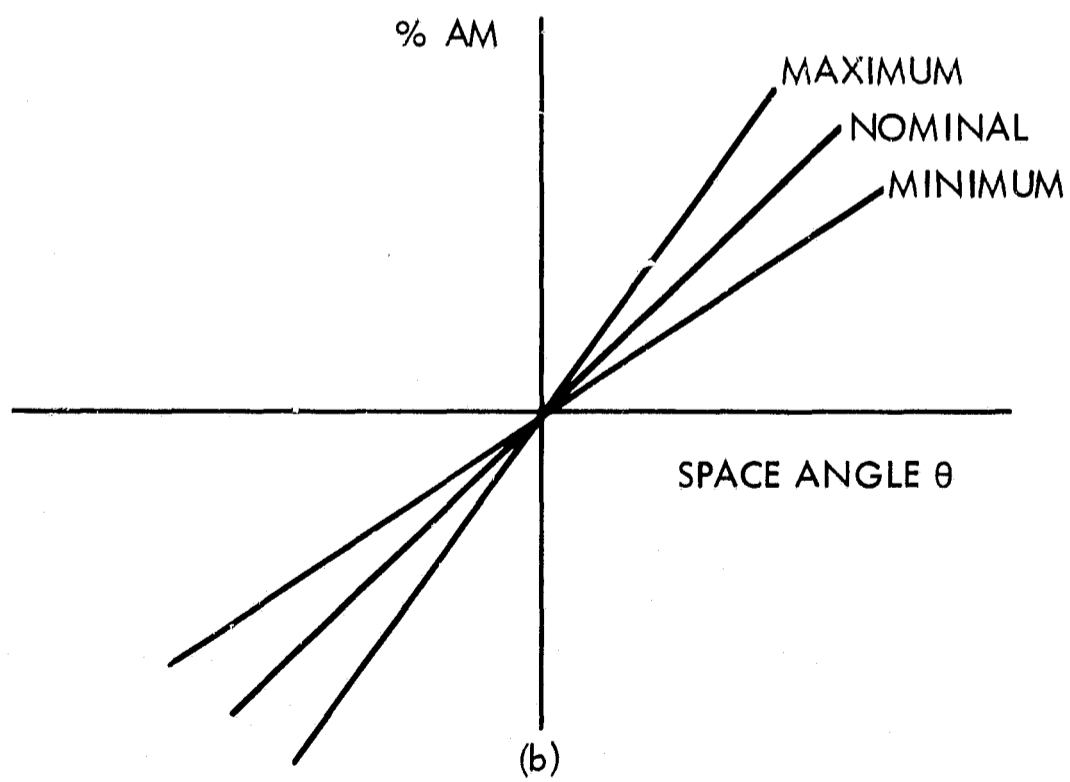
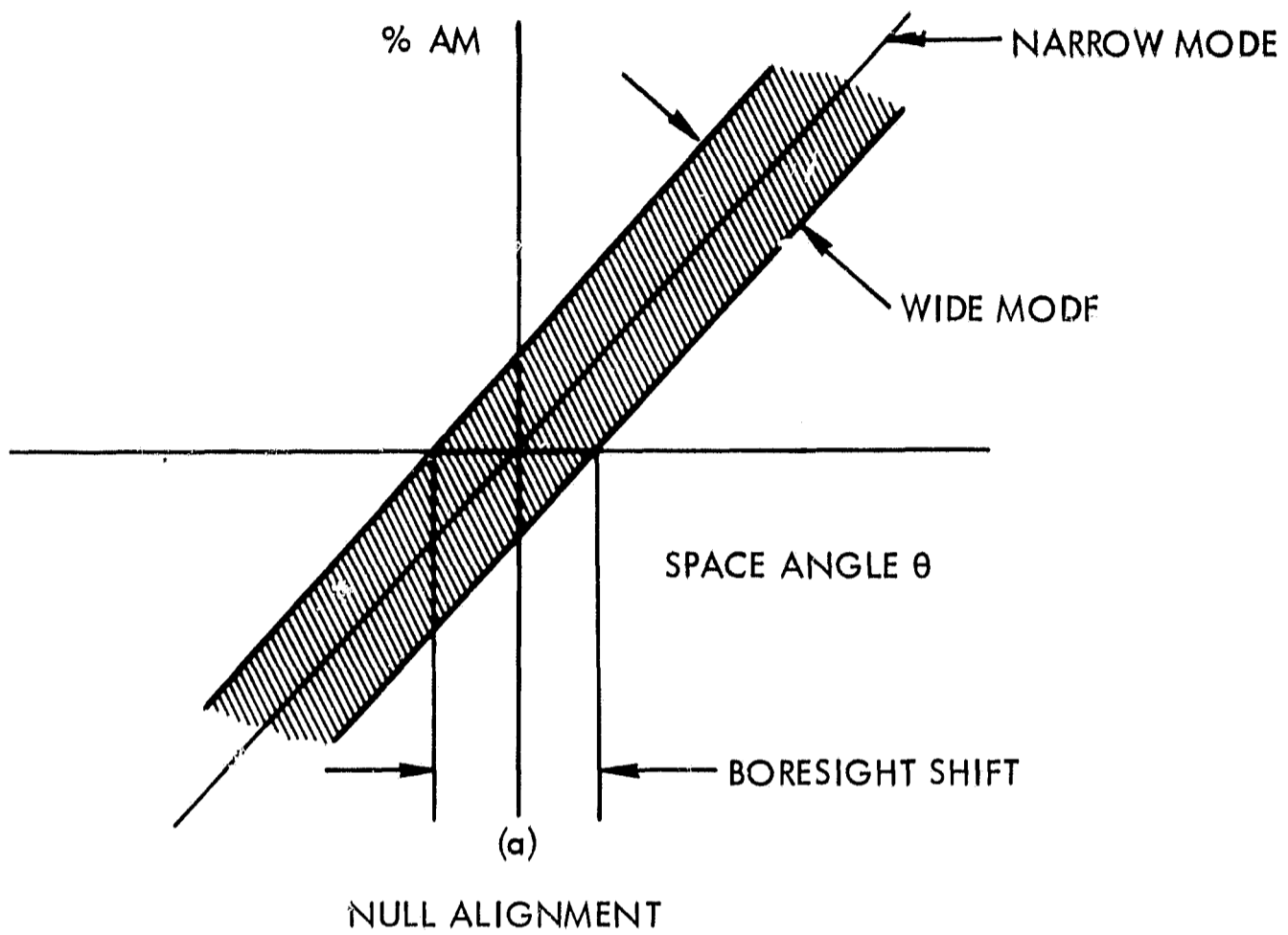
5.1 Format For The Interchangeability Study Output

The output of the study will be a report with boresight and percent modulation information in the form of curves similar to these shown in Figures 8.0 and 9.0. The narrow beam RF boresight will be established as a reference, and broad beam boresight shift will be measured relative to the narrow beam as in Figure 8.0(a). The narrow and broad beam index of modulation variation will be in the form shown in Figures 8.0(b) and 9.0(a) where the maximum, nominal, and minimum antenna gain constants are determined by the respective slopes of the modulation curves. Since both the wide beam boresight and percent modulation slope can vary, an envelope of the wide beam transfer function similar to Figure 9.0(b) will be included. The antennas are tested using two test procedures, and a set of curves is required for each procedure making a total of eight curves.

5.2 Use of the RF Mathematical Model

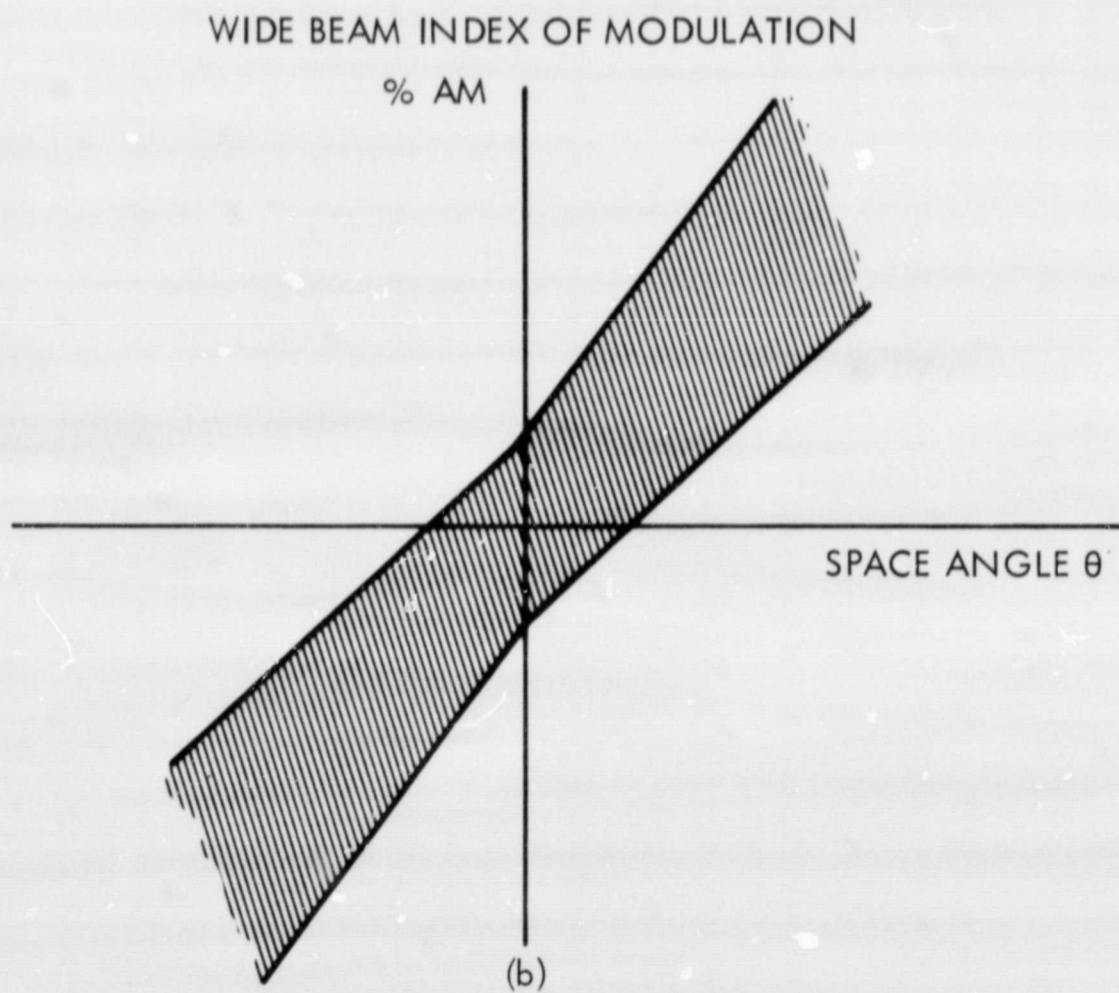
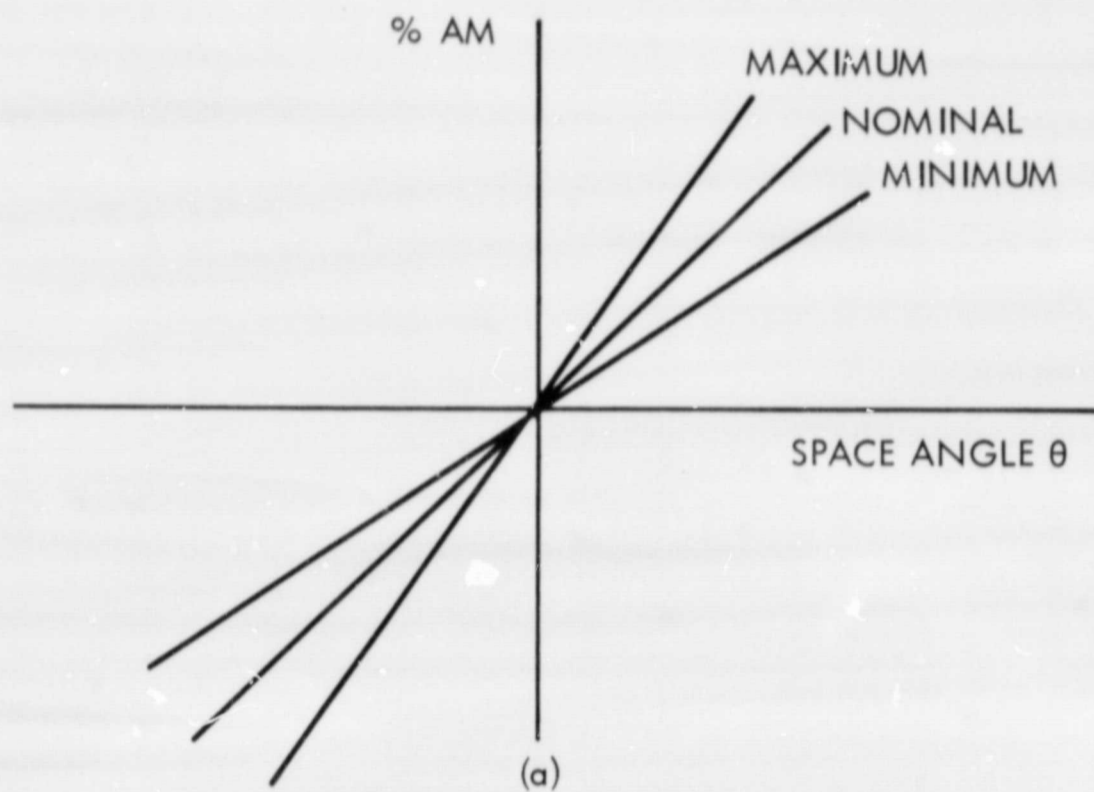
The RF mathematical model will serve three essential functions in arriving at the interchangeability data in paragraph 5.1. These are as follows:

1. Prediction of critical circuit parameters
2. Calculation of the adjustment range of k required to compensate for RF component manufacturing tolerances.
3. Calculation of the boresight shift and percent modulation variation caused by component temperature differentials resulting from the operational environment.



NARROW BEAM INDEX OF MODULATION

Figure 8. Narrow Mode Transfer Functions



WIDE BEAM INDEX OF MODULATION ENVELOPE

Figure 9. Wide Mode Transfer Functions

5.3 Use of the In-Line Test Procedure

The in-line test procedure indicates that the RF component manufacturing tolerances are compensated for by aligning the broad and narrow beam boresight and setting the percent modulation slopes equal. The final transfer function data (in the format of Figures 8. and 9.) will include error contribution from the in-line tests and the mathematical model as indicated in Paragraph 5.2.

6.0 CONCLUSIONS

The purpose of this report has been to present a mathematical model of the RF portion of the HGA system and to establish a method for determining the RF subsystem interchangeability. The RF sub-assembly transfer function of the CSM-HGA system has been accurately expressed mathematically and programmed on TRW's on-line conversational computer (See Appendix for the computer listing). The program uses RF component amplitude and phase unbalances due to manufacturing tolerances to determine the required adjustment range of the coupling coefficient k and calculates the RF subsystem transfer function variations caused by temperature differentials in the operational environment. The model has been reduced to a simplified form for angles near boresight to show the critical parameters that determine antenna gain constant and boresight error. As outlined in Paragraph 5.0, a procedure that utilizes the output of the model and the accuracy of the in-line tests will be used to generate the RF subsystem transfer function envelope. By combining errors due to inaccuracies in the assembly procedures with the transfer function variations derived from the RF math model, an overall transfer function envelope can be derived (See Section 5.0). The results of this analysis will be published in a later report.

Since the CSM HGA RF subsystem is very similar to the lunar module (LM) S-band steerable antenna RF subsystem, the mathematical model may be converted for use in any further LM steerable antenna system tracking studies with minimum added effort.

APPENDIX
MATH MODEL COMPUTER PROGRAM LISTING

The computer program computes the index of modulation as a function of boresight angle for the wide and narrow beam modes with RF component amplitude and phase tolerances as parameters. Antenna element patterns for both modes are included in the program. Crosstalk between modes is also included, with all errors set to zero for the "off" mode. The resultant modulation index is calculated at a $1/3^\circ$ interval over a $\pm 12^\circ$ space angle θ . To provide desired flexibility, provision is made for choosing either wide beam or narrow beam operation for the "on" mode. The coupling constants for each mode can be adjusted separately when required. It is also possible to calculate the modulation index curve of either mode without crosstalk so that the perturbation due to crosstalk may be ascertained.


```

235. PS11=6.28*D/L*HMA*SINH(T)+POA*PF2;
240. PS12=6.28*D/L*HMA*SINH(T)+POR*PR2;
245. RVA2=EA*ECOS(PS11/2.)+KA2*EC*ECOS(PS11/2.);
250. IVA2=EA*SIN(PS11/2.)-KA2*EC*SIN(PS11/2.);
255. RVR2=EB*ECOS(PS12/2.)+KB2*ED*ECOS(PS12/2.);
260. IVR2=EB*SIN(PS12/2.)-KB2*ED*SIN(PS12/2.);
265. VA2=SQRT(RVA2**2.+IVA2**2.);
266. IF IVA2=0. THEN ARGVA2=1.5708; ELSE ARGVA2=-1.5708;
267. IF RVA2=0. THEN GO TO VAT;
270. ARGVA2=ATAN(IVA2./RVA2.);
275. VR2=SQRT(RVR2**2.+IVR2**2.);
276. IF IVR2=0. THEN ARGVR2=1.5708; ELSE ARGVR2=-1.5708;
277. IF RVR2=0. THEN GO TO VBT;
280. ARGVR2=ATAN(IVR2./RVR2.);
285. RVC2=VA2*ECOS(ARGVA2+PTL/2.+PC2/2.)+KC2*V*2*ECOS(ARGVR2+PTL/2.+PC2/2.);
290. IVC2=VA2*SIN(ARGVA2+PTL/2.+PC2/2.)-KC2*V*2*SIN(ARGVR2+PTL/2.+PC2/2.);
295. VC2=SQRT(RVC2**2.+IVC2**2.);
300. ARGVC2=ATAN(IVC2./RVC2.);
305. VDL=K*VD;
310. ARGVDL=ARGVD+1.5708;
315. VSH=KLC*VC2;
320. ARCVSH=ARGVC2+DCL;
325. IF I=0. THEN ARGVDL=ARGVDL+PHI;
326. IF I=0. THEN ARGVSH=ARGVSH+PHI;
327. REVDL=VDL*ECOS(ARGVDL);
330. REVSH=VSH*ECOS(ARGVSH);
335. IMVDL=VDL*SIN(ARGVDL);
340. IMVSH=VSH*SIN(ARGVSH);
345. IF I=1. THEN GO TO FINISH;
346. revdl=REVDL;
347.1. imvdl=IMVDL;
347.2. revsm=REVSH;
347.3. imvsm=IMVSH;
347.4. I=1.;
347.5. KA, KB, KC, KA2, KB2, KC2, KLC=1.2;
347.6. POA, POR, PA, P, PA2, PSM, PD, PA2, PR2, PTL, PC2, DCL, PHI=0.;
350. IF R<1. THEN GO TO SECON; ELSE GO TO NARROW;
355. REVR=REVSH+revdl+revsm;
360. IVR=IMVSH+imvsm+imvdl;
365. VR=SQRT(REVR**2.+IVR**2.);
370. REVL=REVSH+revsm+revdl;
375. IIVL=IMVSH+imvsm+imvdl;
385. VL=SQRT(REVL**2.+IIVL**2.);
390. MI=(VR-VL)/(VR+VL);
395. DCL T DEC(6), MI DEC(6);
400. PUT LIST(H, T);
END LOOP;
6120 END OF PROGRAM LISTING
LOGOUT(OFF)
DATE 88.306 TIME 7:09:28 ( TIME OP WAS 6:49:50 )
USER CLOCKS 8 K: 6:12
TOTAL CPU TIME 0:12
--LOGOUT COMPLETE

```

REFERENCES

1. Skolnik, Merrill I., "Introduction to Radar Systems", McGraw-Hill Book Company, Inc., New York, 1962, pp.182.
2. International Telephone and Telegraph Corporation, "Reference Data for Radio Engineers", American Book - Stratford Press, Inc., New York, 1949, pp. 529.
3. Kraus, John D., "Antennas", McGraw-Hill Book Company, Inc, New York, 1950, pp. 58.
4. Dalmo Victor, "Microwave In-Line Test Procedure for Apollo CSM High Gain Antenna", Report Number 15786, 11 October 1966.
5. Ibid, pp 69.
6. Ibid, pp 78.
7. Ibid, pp 73.